

# Synthesis and Application of a Novel Acid Assisted Hydrochar for Fluoride Contaminated Water Treatment

Endashaw Workie Yihunu, Ying Liu, Chong Chen and Limin Ma\*

College of Environmental Science and Engineering, Tongji University, Shanghai 200092, China.

\*Corresponding author

**Abstract**—In this study, the adsorption behavior of fluoride has been investigated using the biomass derived activated hydrochar (AHC) prepared by a two-stage carbonization process. The adsorption process was spontaneous and exothermic in nature. The adsorption equilibrium data fitted to Langmuir isotherm. The maximum fluoride loading capacity ( $Q_m$ ) of AHC was found to be 88.7 mg/g. The adsorption process was spontaneous and exothermic in nature. Electrostatic interaction between the anion and the positive functional groups in the adsorbent was the main driving force for the adsorption of fluoride. Hence, activated hydrochar can be promising as an effective adsorbent to treat fluoride contaminated water.

**Keywords**—component; fluoride; adsorption; *teff* (*Eragrostis tef*); hydrochar

## I. INTRODUCTION

Biomaterials can widely apply for pollutant removal after their surface introduced the functional groups and carbons via a simple technical route under aqueous medium and relatively low temperature, referred to as hydrothermal carbonization (HTC) process [1]. The presence of such functional groups with its carbonized features on the surface of hydrochar enabled it as a promising precursor for fluoride treatment. Moreover, the suitability of hydrochar can be improved via the chemical assistance such as HCl [2],  $ZnCl_2$  [3],  $H_3PO_4$  [4], etc. The removal of fluoride via phosphoric acid assisted hydrochar derived from *Teff* (*Eragrostis tef*) straw, an agricultural waste, have not yet been reported.

This study explored the removal of fluoride via acid assisted hydrochar prepared from *Teff* (*Eragrostis tef*) straw was investigated. The adsorption kinetic behaviors, and equilibrium isotherm models were analyzed.

## II. MATERIALS AND METHODS

### A. Adsorbents Preparation and Physicochemical Characterization

*Teff* straw was cut into smaller pieces, washed thoroughly, dried, crushed well and sieved. Two stage carbonization process was done as the following method. For pre-carbonization, about 8 g of prepared *Teff* straw was mixed with 56.0 ml of 30 wt%  $H_3PO_4$  solution in a 100 ml Teflon lined autoclave reactor. The reactor was heated at 190°C for 3 h, and

then cool down naturally to room temperature. After the supernatant was removed, the post carbonization process was started through directly transferring the remaining wet solid precursors to a tubular furnace to be pyrolyzed at 450°C for 3h under inert atmosphere. The activated char was taken out after the heat was a cooldown naturally to room temperature. The solid product was washed frequently by a distilled water till the effluent becomes neutral pH. The final char was obtained after dried at 110°C for 6 h.

The surface morphology AHC was observed by Scanning Electron Microscope at 15 kV accelerating voltage (SEM, JSM-7800F). The presence of functional groups on the surfaces was confirmed by Fourier Transform Infrared Spectroscopy (FTIR, Nicolet IS 10) in a wavelength of 400 to 4000  $cm^{-1}$ . The textural feature of both adsorbents was determined by  $N_2$  adsorption-desorption isotherms at 77 K using ASAP (Micrometrics 2460) surface area and porosity analyzer. Subsequently, the surface area and average pore size were calculated by the Brunauer-Emmett-Teller (BET) and Barret-Joyner-Halenda (BJH) method, respectively.

### B. Adsorption Experiment

A standard fluoride solution was obtained by dissolving 0.221 g anhydrous NaF in distilled water and then diluted to the required concentration. A series of the batch experiment was done to investigate the best conditions of adsorption parameters. Accordingly, 0.1 g of AHC was added in 20 mg/l of 100 ml fluoride solution with variable pH (2–12), agitated for 3 h at a 25°C. Subsequently, the variation effect of adsorbent dose (0.1–1 g) was studied. Thermodynamic properties of the adsorbent-adsorbate reaction were evaluated at variable temperatures (288–328 K). The adsorption kinetics was also studied by measure the residual fluoride concentration at different adsorption time intervals (15–300 min). Prior to fluoride determination, the supernatant was filtered and then mixed equally with TISAB II solution to avoid the ionic interference during the fluoride measurement. The remained concentrations of fluoride were measured twice by benchtop ion meter with a fluoride ion selective electrode (PXSJ-216F, China) and the average result was used for analysis.

The amount of fluoride uptake was calculated using the mass balance equation (1):

$$\text{Adsorption capacity } (Q_e) = (C_i - C_0)V/W \quad (1)$$

where V is the volume of solution, W is the weight of adsorbent (g),  $C_i$  (mg/l) and  $C_e$  (mg/l) are the initial and equilibrium fluoride concentrations (mg/l), respectively.

### III. RESULTS AND DISCUSSION

#### A. Physicochemical Properties of the Adsorbent

SEM images in FIG. I depicted the structural properties of AHC. The AHC displayed dominantly exhibited a rough coalesced carbon layer with stacked alignment. During the HTC process, the acidic medium has gradually seeped into the amorphous cellulose and some soluble segments of lignin of straw resulting to cracked and disrupt the cellulose chain (Lei et al., 2018).

According to IUPAC classification, AHC exhibited isotherm type IV with H3 hysteresis loop, indicating staged adsorption on mesopores. Its hysteresis loop revealed loose assemblages of the plate-like structure at which the capillary condensation taking place to fill and withdraw  $N_2$  molecules on those mesopores. The BET specific surface area and total pore volume (VT) of AHC is  $43.8 \text{ m}^2\text{g}^{-2}$  and  $0.087 \text{ m}^3\text{g}^{-1}$ . The linkages of phosphate and phosphate ester with lignocellulose may encourage the expansion of the structure, whereby the void volume was protected [5].

The FTIR results shows peaks at  $3421 \text{ cm}^{-1}$  and  $1036 \text{ cm}^{-1}$  which are assigned to stretching vibrations of O-H [6] and sulfonic group, respectively. The peak observed at  $2908 \text{ cm}^{-1}$  derived from the asymmetric aliphatic saturated C-H group and  $1632 \text{ cm}^{-1}$  indicating C=C stretching vibrations and its derived carbons [7]. A weak band were also observed at  $609 \text{ cm}^{-1}$ , indicating the presence of C-C stretching.

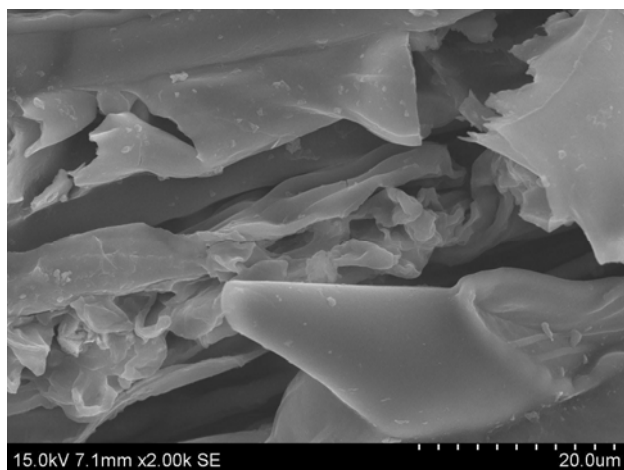


FIGURE I. SEM IMAGES OF AHC.

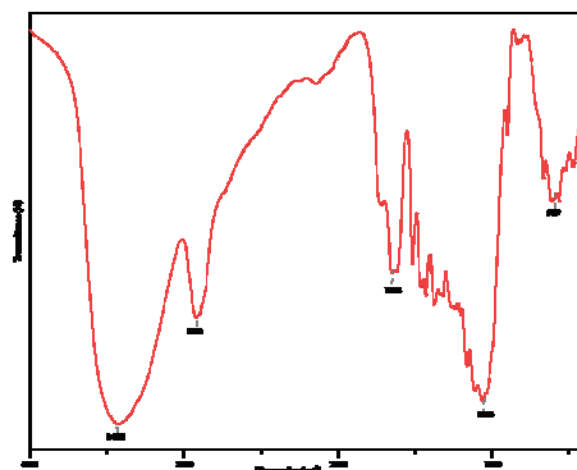
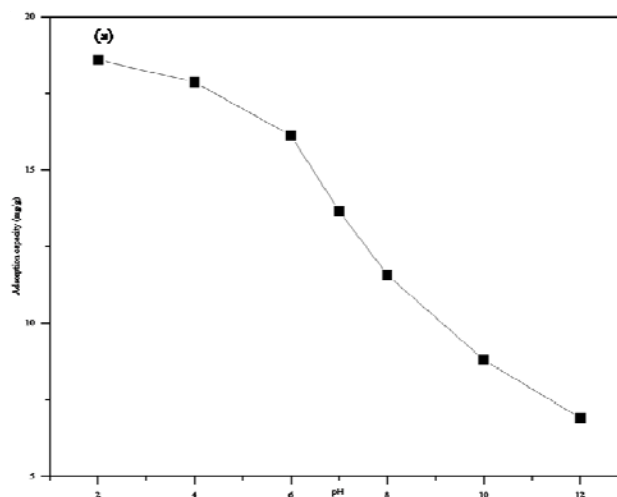


FIGURE II. FTIR SPECTRA OF AHC.

#### B. Effects of the Solution pH and Adsorbent Dose

High adsorption capacity was recorded in low pH with a peak at pH 2 while abruptly ceased after pH 8 (FIG. IIa). It is evident that the presence of  $H^+$  at low pH, the attraction of fluoride ion with the adsorbent sites could be strengthened since the hydroxylation process is formed [8]. Conversely, the higher pH enhances the adsorption competition between hydroxyl and fluoride ions, thereby the adsorbent sites could be more occupied by hydroxide ions over aimed adsorbate.

In order to examine the effect of adsorbent dose, 100 mg/l of initial fluoride solution was employed with an adsorbent dose started from 0.1 to 1.1 g. The result shows decreasing the fluoride concentration with increasing in adsorbent dose (FIG. IIb). This phenomenon may be due to the difference in the availability of free active sites which still enabled to adsorb the remaining ions.



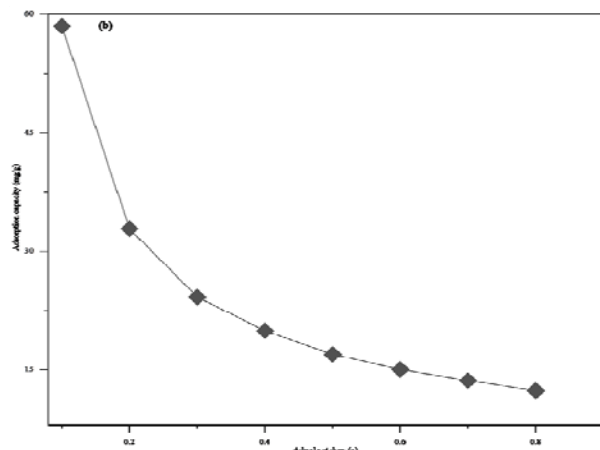


FIGURE III. EFFECTS OF PH OF THE SOLUTION (A) AND HTS DOSE (B).

### C. Adsorption Isotherm

The adsorption response for an increment in the amount of adsorbate at constant temperature was studied. Langmuir and Freundlich isotherm models were used (Table I). The Langmuir isotherm fitted with the experimental data ascribing the adsorption process take place on their surface with limited interaction of adsorbed molecules. The maximum monolayer adsorption capacity  $Q_m$  of AHC at 100 mg/L were found to be 88.7 mg/g.

TABLE I. THE LANGMUIR AND FREUNDLICH ISOTHERM MODEL PARAMETERS

Initial F <sup>-</sup> Concentration	Langmuir			Freundlich	
	$q_m(\text{mg/g})$	$K_L(\text{L/mg})$	$R^2$	$K_f(\text{mg/g})$	$R^2$
100 mg/l <sup>a</sup>	88.7	0.12	0.96	4.7	0.91

a. initial fluoride concentration

### D. Adsorption Kinetics

The adsorption experimental data was correlated using the pseudo-first-order and pseudo-second-order kinetic models. Based on the higher correlation coefficients along with a close value of experimental and calculated adsorption capacity, the pseudo-second-order ( $R^2=0.97$ ) were favorably fitted by the pseudo-second-order model than the pseudo-first-order. Thus, the adsorption of fluoride onto both adsorbents were governed by chemical reaction at which the electrons are shared between adsorbent sites and fluoride ions via valency forces.

### E. Thermodynamic Studies

AHC was exhibited the spontaneous adsorption process and the exchange is proportional to the temperature of the solution. The positive values of change in enthalpy revealed an exothermic adsorption process. It also likely indicated the higher electronegativity of fluoride ion and its substitution for hydroxide ion on the carbonized feature of the adsorbents, thereby chemical in nature. Moreover, the positive values of change in entropy confirm the affinity of fluoride ions towards the adsorbents.

## IV. CONCLUSIONS

A phosphoric acid assisted hydrochar were successfully produced by hydrothermal carbonization process. The morphological, textural, crystal and chemical characterization was proven its favorable adsorbent features. The pH of the solution and amount of adsorbent affected significantly the adsorption process. The adsorption kinetics fitted pseudo-second-order, indicating the chemisorption process. The experimental result confirmed activated hydrochar as an efficient adsorbent to treat a fluoride contaminated water.

## ACKNOWLEDGMENT

The This work was supported by the Key Program of China (2018YFC1803103, 2017ZX07206) and National Natural Science Foundation of China (No. 21377098).

## REFERENCES

- [1] Q. Xu, Q. Qian, A. Quek, N. Ai, G. Zeng, and J. Wang, "Hydrothermal carbonization of macroalgae and the effects of experimental parameters on the properties of hydrochars," ACS Sustain. Chem. Eng., vol. 1, no. 9, pp. 1092–1101, 2013.
- [2] W.-C. Qian, X.-P. Luo, X. Wang, M. Guo, and B. Li, "Removal of methylene blue from aqueous solution by modified bamboo hydrochar," Ecotoxicol. Environ. Saf., vol. 157, pp. 300–306, Aug. 2018.
- [3] H. Zhang, Y. Yan, and L. Yang, "Preparation of activated carbon from sawdust by zinc chloride activation," Adsorption, vol. 16, pp. 161–166, 2010.
- [4] S. M. Yakout and G. Sharaf El-Deen, "Characterization of activated carbon prepared by phosphoric acid activation of olive stones," Arab. J. Chem., vol. 9, pp. S1155–S1162, 2016.
- [5] A. Kundu, B. Sen Gupta, M. A. Hashim, and G. Redzwan, "Taguchi optimization approach for production of activated carbon from phosphoric acid impregnated palm kernel shell by microwave heating," J. Clean. Prod., vol. 105, pp. 420–427, Oct. 2015.
- [6] L. Hongtao, Liu Shuxia, Zhang Hua, et al., "Comparative study on synchronous adsorption of arsenate and fluoride in aqueous solution onto MgAlFe-LDHs with different intercalating anions," RSC Adv., pp. 33301–33313, 2018.
- [7] H. Sano, K. Omine, M. Prabhakaran, A. Darchen, and V. Sivasankar, "Groundwater fluoride removal using modified mesoporous dung carbon and the impact of hydrogen-carbonate in borehole samples," Ecotoxicol. Environ. Saf., vol. 165, pp. 232–242, Dec. 2018.
- [8] B. D. Gebrewold, P. Kijjanapanich, E. R. Rene, P. N. L. Lens, and A. P. Annachhatre, "Fluoride removal from groundwater using chemically modified rice husk and corn cob activated carbon," Environ. Technol. (United Kingdom), vol. 0, no. 0, pp. 1–15, 2018.